$Bi_2Sr_2CaCu_2O_{8+\delta}$ Bicrystal c-Axis Twist Josephson Junctions: A New Phase-Sensitive Test of Order Parameter Symmetry

Qiang Li,[1] Y. N. Tsay,[1] M. Suenaga,[1] R. A. Klemm,[2] G. D. Gu,[3,*] and N. Koshizuka[3]

[1]*Department of Applied Science, Brookhaven National Laboratory, Upton, New York 11973*
[2]*Materials Science Division, Argonne National Laboratory, Argonne, Illinois 60439*
[3]*Superconductivity Research Laboratory, ISTEC, 10-13, Shinonome 1-chome, Koto-ku, Tokyo, 135, Japan*
(Received 6 July 1999)

We prepared atomically clean $Bi_2Sr_2CaCu_2O_{8+\delta}$ Josephson junctions between identical single crystal cleaves stacked and twisted an angle ϕ_0 about the c axis. For each bicrystal, the ratio J_c^J/J_c^S of the c axis twist junction critical current density to that across either single crystal part is unity, independent of ϕ_0 and the ratio A^J/A^S of junction areas. Our results provide strong evidence for incoherent c-axis tunneling and that the dominant superconducting order parameter contains an isotropic s-wave component for $T \lesssim T_c$, but not the purported $d_{x^2-y^2}$-wave component.

There has long been a raging controversy over the orbital symmetry of the superconducting order parameter (OP) in high transition temperature T_c superconductors. For pairing within the nominally tetragonal CuO_2 layers, the C_{4v} point group allows the spin singlet OP eigenfunctions denoted s, $d_{x^2-y^2}$, d_{xy}, and $g_{xy(x^2-y^2)}$, relative to the planar Cu-O bond directions [1,2]. In the lattice representation, where $\mathbf{k} = (k_x, k_y)$ and $|k_x|, |k_y| \leq \pi/a$ in the first Brillouin zone (BZ), these, respectively, group transform as a constant, $\cos(k_x a) - \cos(k_y a)$, $\sin(k_x a)\sin(k_y a)$, and $\sin(k_x a)\sin(k_y a)[\cos(k_x a) - \cos(k_y a)]$, each multiplied by some function $\sum_{n,m} a_{nm}\cos(nk_x a)\cos(mk_y a)$ with $a_{nm} = a_{mn}$ [2]. Phase-sensitive experiments can distinguish a $d_{x^2-y^2}$ OP, with nodes at $k_x = \pm k_y$, from an "extended-s" OP, $\{[\cos(k_x a) - \cos(k_y a)]^2 + \epsilon^2\}^{1/2}$ ($\epsilon \ll 1$).

Most experiments were performed on orthorhombic $YBa_2Cu_3O_{7-\delta}$ (YBCO). The C_{2v}^1 point group allows the mixed $s + d_{x^2-y^2}$ OP, in agreement with most phase-sensitive experiments [1–4]. However, some experiments suggest a larger $d_{x^2-y^2}$ component [3,4], but others suggest a larger s component, with a nodeless OP [5,6]. Also, nonsuperconducting gaps appear to be present above and below T_c, complicating the analysis [6,7].

In orthorhombic $Bi_2Sr_2BaCu_2O_{8+\delta}$ (Bi2212), the bc plane containing a diagonal between the Cu-O bond directions and the periodic lattice distortion $\mathbf{Q}$ is a crystallographic mirror plane [8,9]. The C_{2v}^{13} point group allows mixed $s + d_{xy}$ and $d_{x^2-y^2} + g_{xy(x^2-y^2)}$ OPs, but the *incompatible* s and $d_{x^2-y^2}$ components can mix only below an unobserved second phase transition at $T_{c2}^< < T_c$ [1,2].

Recent Bi2212/Pb c-axis Josephson junction experiments showed that Bi2212 has at least a small isotropic s-wave OP component below $T_c^{Pb} = 7.2$ K [10], as did similar experiments with Pb and thin films of $Nd_{1.85}Ce_{0.15}CuO_4$, generally thought to have an isotropic s-wave OP, or YBCO [11]. If the dominant Bi2212 OP component were $d_{x^2-y^2}$, a nodeless OP

such as $d_{x^2-y^2} + is$ would result below $T_{c2}^< > T_c^{Pb}$. If $T_{c2}^< \ll T_c$, this might not affect phase-insensitive experiments such as angle-resolved photoemission spectroscopy (ARPES) and penetration depth measurements [12,13], which suggest an OP with nodes or near nodes. Thus, it is crucial to determine if the s-wave component is present at T_c. Also, those experiments might be complicated by nonsuperconducting gaps, whereas Josephson tunneling involves only the OP. Here we describe exceedingly clean, novel phase-sensitive Josephson junction experiments, giving strong evidence that the s-wave OP component is indeed present at T_c.

Very high quality single crystals of Bi2212 were prepared by the traveling solvent floating zone technique, and cut into smaller pieces, which were cleaved in the ab plane in air. One cleave was rotated a desired angle ϕ_0 about the c axis with respect to the other, and placed atop it. The twist boundary was formed in a controlled sintering process for 30 hours in air or controlled oxygen pressure, just below the melting point of Bi2212. Depending upon the atmosphere and the subsequent annealing, optimally doped or overdoped samples could be obtained, with T_c varying from 90 to 80 K, respectively. The resulting c-axis twist junctions were examined using conventional and high resolution transmission electron microscopy (HRTEM), electron energy-loss spectroscopy, and energy dispersive x-ray spectroscopy, and found to be atomically intact and clean over the entire areas studied ($\approx 10^2$ μm^2), with no detectable c-axis spacing increase or chemical changes between the BiO double layers [8]. An optical micrograph of a resulting 45° c-axis twist bicrystal with six leads attached is pictured in Fig. 1a. Note that the area A^J of the twist junction is about half the cross-sectional area A^S of the identical single crystal cleaves.

A schematic side view of the bicrystal with leads attached is sketched in Fig. 1b. Electrical contacts were made by first sputtering six Ag pads (≈ 1 μm thick) with subsequent annealing in pure O_2 at 570 °C for about
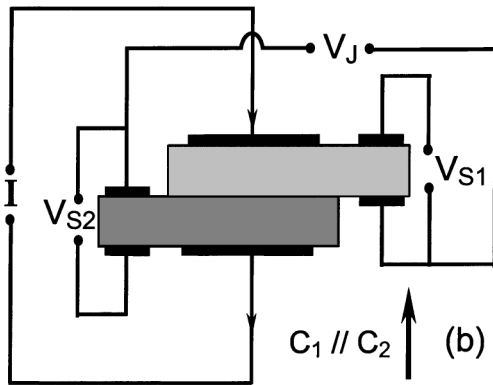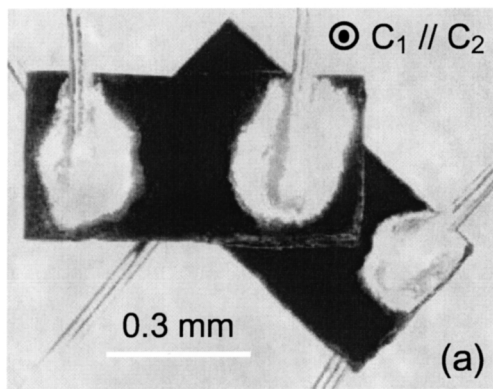
FIG. 1.   (a) Top view photomicrograph of a 45° c-axis twist junction (sample H) with six attached electrical leads. (b) Sketch of a side view of the bicrystal, with six attached leads.

10 min. 0.002" Au wires were attached to the pads with Ag epoxy. Current I was fed along the common c axis, and the voltages V_{s1} and V_{s2} were measured across each single crystal cleave. The voltage V_J across the twist junction was measured from the bottom lead on the top crystal to the top lead on the bottom crystal. This configuration allows us to measure simultaneously the c-axis V-I characteristics across either single crystal cleave and the twist junction. The measurements were made at zero field in a magnetically shielded apparatus (the remnant field was <10 mOe) with a temperature T control accurate to 0.01 K.

Figure 2 shows the hysteretic V-I characteristics of a $\phi_0 = 45°$ twist junction at 10 K, demonstrating its Josephson behavior. This sample was subsequently destroyed by overheating during a V-I measurement at 5 K. In the inset of Fig. 3a, a semilog V-I plot of the characteristics at 50 K of the $\phi_0 = 50°$ twist junction and a constituent single crystal of sample J is shown. I was turned off immediately after the resistive transition of the twist junction was observed to avoid such overheating. By applying $\mathbf{I} \| \hat{\mathbf{c}}$ and measuring V, the c-axis critical currents I_c^i for the twist junction ($i = J$) and for the single crystal ($i = S$) in the superconducting state were easy to identify, since the voltage jumps were more
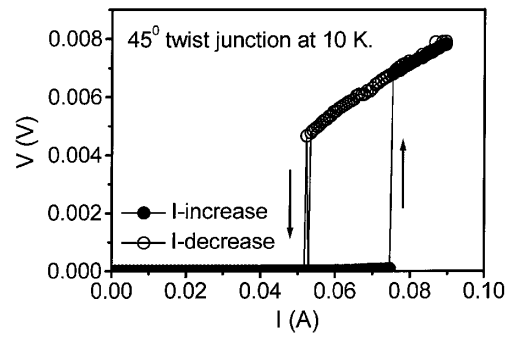
FIG. 2.   Hysteretic V-I plot at 10 K for a 45° c-axis twist junction (sample Q13-99).

than 4 and 8 orders of magnitude, respectively, as shown. From the data shown in Fig. 2 and the inset of Fig. 3a, $R_n(T)$ can be approximated by the slope of V just above $I_c^J(T)$. Although the $I_c^J(10 \text{ K})$ for these samples differ by only $\approx 15°$, $R_n(10 \text{ K}) \gg R_n(50 \text{ K})$. This strong c-axis $R_n(T)$ dependence has been observed previously [14].

We attempted to observe a Fraunhofer pattern in a parallel field [4], but were unsuccessful, since Bi2212 is intrinsically a stack of coupled Josephson junctions [15]. To observe a Fraunhofer pattern, one has to make uniform twist junctions much weaker than the intrinsic single crystal ones, yet equal in strength in each bicrystal.
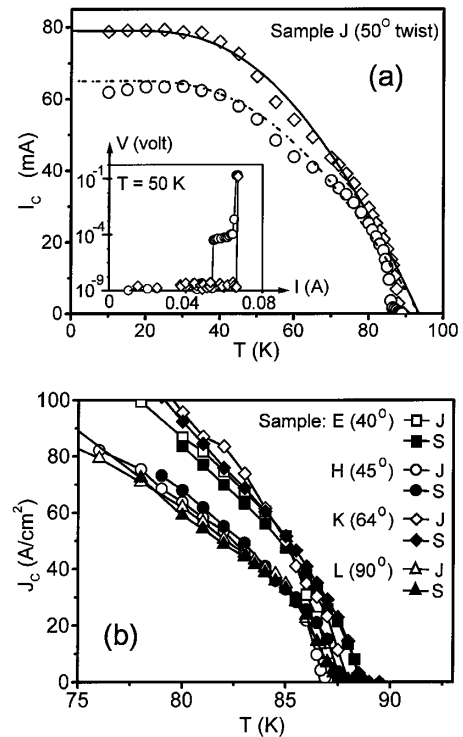
FIG. 3.   (a) $I_c^i(T)$ data for $i = S$ ($\diamond$) and $i = J$ ($\circ$) obtained from sample J ($\phi_0 = 50°$), along with AB fits (curves). Inset: Semilog $V - I$ plot at 50 K. (b) $J_c^i(T) = I_c^i(T)/A^i$ data for samples E, H, K, and L, with $\phi_0 = 40°, 45°, 64°$, and $90°$ for 75 K $<T< T_c$. Solid: J_c^S. Open: J_c^J. Lines are eye guides.

For each of the 12 bicrystals studied, we measured the superconducting onset T_c, the twist angle ϕ_0, the cross-section areas A^i, and the corresponding $I_c^i(T)$ for $T_{\min}^i \leq T \leq T_c$, where $T_{\min}^i < 0.9T_c$, for $i = J, S$. For each bicrystal, $I_c^J(0.9T_c) < I_c^S(0.9T_c)$, and A^J/A^S varies from 0.85 to 0.24. Hence, the relevant quantities for comparison are the critical current densities $J_c^i = I_c^i/A^i$ at the same T/T_c value. In Table I, we list these ϕ_0, T_c, A^i, and $I_c^i(0.9T_c)$ values for $i = J, S$, and the ratios J_c^J/J_c^S at $0.9T_c$. Although each $J_c^i(0.9T_c)$ value is distinct, except for sample B, each of these J_c^J/J_c^S ratios ≈ 1. The remarkable independence of J_c^J/J_c^S on both A^J/A^S and ϕ_0 demonstrates that the junctions are indeed very uniform.

In some samples, the A^i were small enough that the $I_c^i(T)$ could be measured over the entire range 10 K $\leq T \leq T_c$. In Fig. 3a, we plotted the $I_c^i(T)$ data obtained from sample J ($\phi_0 = 50°$), along with the Ambegaokar-Baratoff (AB) fits [16]. Clearly, our results are consistent with the AB model. In Fig. 3b, we plotted $J_c^i(T) = I_c^i(T)/A^i$ for $i = J, S$ in the vicinity of T_c for samples E(40°), H(45°), K(60°), L(90°). Except for a narrow region $\Delta T_{Ji} \approx 1$ K at the onset of $J_c^i(T)$, $J_c^S(T)$ and $J_c^J(T)$ are indistinguishable for each sample. Below $T_c - \Delta T_{Ji}$, $J_c^i(T) \propto (T_{c0} - T)$ is mean-field-like, where $T_{c0} = T_c + \Delta T_c$, where $\Delta T_c \approx 3$ K. Hence, superconducting fluctuations affect the J_c^i only within the narrow range $T_c - \Delta T_{Ji} \leq T \leq T_{c0}$.

Sample B has a lower J_c^J/J_c^S ratio at $0.9T_c$ than the other samples. Although we have not explicitly examined sample B with HRTEM, we suspect that it might have been damaged when attaching the contact leads prior to the transport measurements. Nevertheless, we measured its $I_c^i(T)$ from 25 K to T_c, and the $I_c^i(T)/I_c^i(0)$ were identical to those of the other samples.

For weak tunneling between adjacent layers 1 and 2, $J_c^i = |4eT \sum_\omega \langle f^i(\mathbf{k} - \mathbf{k}')F_1(\mathbf{k}_i)F_2(\mathbf{k}_i')\rangle_{1\cap2}|$ for $i = J, S$, where $\mathbf{k}_S = \mathbf{k}$, $\mathbf{k}_S' = \mathbf{k}'$, but $\mathbf{k}_J = \mathbf{k}_+$ and $\mathbf{k}_J' =$

$\mathbf{k}_-'$ are rotated by $\pm\phi_0/2$ about the c axis, respectively. $\langle\cdots\rangle_{1\cap2}$ is an integral over the overlapping first BZs, and $f^i(\mathbf{q})$ is the spatial average of the quasiparticle tunneling matrix element squared [2]. For $n = 1, 2$ and J_c^i to $\mathcal{O}(f^i)$, $F_n = \Delta_n/[\omega^2 + \xi_n^2 + |\Delta_n|^2]$, where ω is a Matsubara frequency, and the quasiparticle dispersions ξ_n and OPs Δ_n are *independent* of the f^i. Bloch's theorem and group theory require $\xi_1(\mathbf{k}_i), \xi_2(\mathbf{k}_i')$ and each component of $\Delta_1(\mathbf{k}_i), \Delta_2(\mathbf{k}_i')$ to lock onto the local Cu-O bond orientation. Although $f^i(\mathbf{q})$ can contain both coherent ($\mathbf{q} = 0$) and incoherent ($\mathbf{q}$ arbitrary) parts, for purely incoherent tunneling (AB), $f^i(\mathbf{q}) = f_0^i$, $\langle F_1 \rangle = \langle F_2 \rangle$, and each $J_c^i = 0$, *except* for an s-wave OP, projecting out its Fermi surface (FS) average near T_c [16].

In Fig. 4, we plotted the $J_c^J(\phi_0)/J_c^S$ data at $0.9T_c$, and compared them with the coherent tunneling predictions $|\cos(\ell\phi_0)|$ for pure s-, p-, and d-wave superconductors [e.g., $\Delta(\mathbf{k}) = \Delta_0\cos(\ell\phi)$, with $\ell = 0, 1, 2$, respectively] in the angular momentum (ℓ), or FS restricted, representation, appropriate for a cylindrical FS on which $k_x = k_F\cos\phi$, etc. As noted above, the curve labeled s also fits an anisotropic s-wave OP with purely incoherent tunneling in any representation. However, symmetry requires that a d-wave OP has $J_c^J(45°) = 0$. More generally, unless the FS average of the s-wave OP component is nonvanishing, $J_c^J(\phi_0^*) = 0$ for some ϕ_0^* [2]. This experiment is thus phase sensitive. The standard deviations of the fits are found to be 0.27, 0.50, and 0.79, respectively. Eliminating sample B changes these to 0.06, 0.46, and 0.81, respectively. Clearly, the fit to the s curve is the best, and the fits to the p and d curves are unacceptably poor. We thus deduce (1) the OP has an s-wave component with a nonvanishing FS average near T_c.

Previously, it was shown that for $T \approx T_{c2}^< < T_{c2}$, the bare transition temperature of a secondary, incompatible OP with d_{xy}- or s-wave symmetry, corrections to the J_c^i of second order in the f^i could allow a predominantly $d_{x^2-y^2}$-wave OP to twist in order to compensate for the junction twist [2]. However, for $T_{c2} < T < T_c$ and the $f^i \to 0$, appropriate for Bi2212, $J_c^J(45°) \approx 0$ close to

TABLE I. c-Axis twist junction ($i = J$) and single crystal ($i = S$) data. S: Sample. A^i: cross-sectional areas. I_c^i: c-Axis critical currents at $0.9T_c$. $J_c^i = I_c^i/A^i$: critical current densities at $0.9T_c$.

S	ϕ_0 (deg)	T_c (K)	A^J (10^{-8} m²)	I_c^J (mA)	A^S (10^{-8} m²)	I_c^S (mA)	J_c^J/J_c^S
A	0	81	10.4	152	22.4	350	0.94
B	25	90	3.1	1.98	3.7	36	0.12
C	27	88.5	9.5	62	12.1	69.8	1.08
D	40	90	6.15	53.3	7.79	65.1	1.04
E	40	89	5.2	48	12.4	123	0.93
F	45	81.5	13.76	171	25	285	1.09
G	45	90	4.26	34	17.94	147	0.97
H	45	90	7.3	46.5	14.8	98	0.96
I	45	90.5	7.5	47	13.6	79.3	1.07
J	50	89.5	2.98	25.3	3.5	29.6	1.00
K	64	91.5	5.47	53.5	7.7	71.5	1.05
L	90	89	8.06	50	17.6	106	1.03
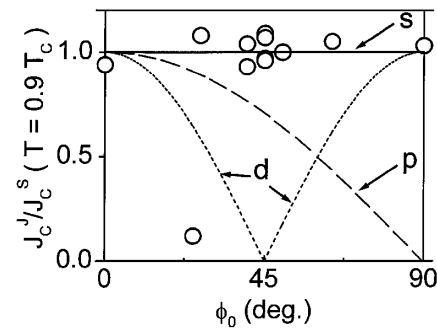
FIG. 4. Plot of $J_c^J(0.9T_c)/J_c^S(0.9T_c)$ data (open symbols) for samples A–L (see Table I) as a function of ϕ_0 (deg). Also shown: theoretical curves for s-wave (solid line), p-wave (dashed curve), and d-wave (dotted curve) order parameters.

T_c. Our experiments thus rule out OP twisting, *unless* $T_{c2}^{<} \approx T_c$. In that unlikely case, the bulk OP would break time-reversal invariance and be nodeless for $0 \leq T < T_{c2}^{<} \approx T_c$, contradicting other experiments [12,13].

We note that if the FS were cylindrical and $f^J(\mathbf{q})$ were coherent, then these experiments would infer an isotropic s-wave OP. However, this scenario is unlikely, since the FS is tight binding, $0 = \xi(\mathbf{k}_F)$, where $\xi(\mathbf{k}) = -t[\cos(k_x a) + \cos(k_y a)] + t' \cos(k_x a) \cos(k_y a) - \mu$ [12,17]. The dominant coherent tunneling processes involve quasiparticle states near the FSs on each side of the junction. Since the intersection of tight-binding FSs twisted $\pm \phi_0/2$ about the c axis is vanishingly small, c-axis twisting reduces such coherent processes. In such a scenario, J_c^J/J_c^S would be largest for $\phi_0 = 0, 90°$, even for an isotropic s-wave OP. Quantitatively, for $f^J(\mathbf{q}) = f_0^J \exp(-\mathbf{q}^2/\sigma)$ and an s-wave OP isotropic on the tight-binding FS, we find substantial $J_c^J(\phi_0)$ variation with coherent ($\sigma = 0$) tunneling, but no noticeable variation for $\sigma \geq \sigma_0 = \frac{1}{4}(\pi/a)^2$ [2]. Since a ϕ_0-independent J_c^J/J_c^S is observed, we deduce (2) the c-axis tunneling across the twist junction is *strongly incoherent*.

For $f^J(\mathbf{q}) = f_0^J \exp(-\mathbf{q}^2/\sigma)$ with a $d_{x^2-y^2}$ OP, increasing σ from 0 to σ_0 reduced J_c^J at $\phi_0 = 0$ by only $\approx 50\%$ [2]. Thus, a highly anisotropic s-wave OP would yield an anisotropic $J_c^J(\phi_0)$ for $\sigma \leq \sigma_0$. Hence (3) in addition to (1) and (2), either (a) the OP is *isotropic* on the FS or (b) the tunneling is *purely* incoherent (AB).

Since $J_c^J = J_c^S$ (4), the twist and intrinsic single crystal junctions are *essentially identical*, $f^S(\mathbf{q}) = f^J(\mathbf{q})$. Except for sample B, HRTEM combined with computer simulations determined that the twist and intrinsic single crystal junctions of our samples, including sample A (0°), are chemically identical, with identical c-axis spacings (15 Å) between the van der Waals–bonded BiO double layers [8]. If the tunneling involved specific atoms in the CuO_2 planes across the junction, a lateral translation of 1 Å across a 45° twist junction would negligibly (by 0.03 Å) increase the tunneling distance d_t. Thus, both the tunneling potential and d_t are ϕ_0 independent. Resonant tunneling, in which the quasiparticles are temporarily trapped within the junction, losing all memory of their parallel momenta, is important for large d_t, similarly insensitive to ϕ_0, and could contribute to the incoherent tunneling [18]. Hence, we can't rule out scenario (3b).

We made Bi2212 bicrystal c-axis twist Josephson junctions of extraordinary high quality. The ratio J_c^J/J_c^S of critical current densities at $T/T_c = 0.9$ across the twist junction to that across the single crystal is unity, independent of the twist angle ϕ_0 and of the ratio A^J/A^S of junction areas. When measurable to low T,

$J_c^J(T) = J_c^S(T)$, and the $J_c^i(T)/J_c^i(0)$ quantitatively fit the AB model, except within a few K of T_c, due to superconducting fluctuations. We conclude that the OP contains an s-wave component with a nonvanishing FS average for $T \leq T_c$, the c-axis tunneling is strongly incoherent, and the twist and intrinsic junctions are essentially identical. In addition, either the OP is isotropic on the FS or the tunneling is purely incoherent. Group theory thus rules out a $d_{x^2-y^2}$-wave component, except possibly below a second, unobserved phase transition at $T_{c2}^{<} < T_c$.

---

*Present address: School of Physics, The University of New South Wales, Kensington, New South Wales, Australia 2033.

[1] J. Annett, N. Goldenfeld, and A. J. Leggett, in *Physical Properties of High Temperature Superconductors V,* edited by D. M. Ginsberg (World Scientific, Singapore, 1996), pp. 375–461.

[2] R. A. Klemm, C. T. Rieck, and K. Scharnberg, Phys. Rev. B **58**, 1051 (1998); cond-mat/9811303 (to be published); R. A. Klemm *et al.,* Phys. Rev. B **58**, 14 203 (1998); J. Low Temp. Phys. (to be published).

[3] C. C. Tsuei *et al.,* Phys. Rev. Lett. **73**, 593 (1994).

[4] K. A. Kouznetsov *et al.,* Phys. Rev. Lett. **79**, 3050 (1997).

[5] A. Bhattacharya *et al.,* Phys. Rev. Lett. **82**, 3132 (1999).

[6] J. Demsar *et al.,* Phys. Rev. Lett. **82**, 4918 (1999); V. V. Kabanov *et al.,* Phys. Rev. B **59**, 1497 (1999).

[7] K. Gorny *et al.,* Phys. Rev. Lett. **82**, 177 (1999).

[8] Y. Zhu *et al.,* Phys. Rev. B **57**, 8601 (1998); Y. Zhu *et al.,* Microsc. Microanal. **3**, 423 (1997).

[9] Y. N. Tsay *et al.,* in *Superconducting Superlattices II: Native and Artificial,* edited by I. Bozovic and D. Pavuna, SPIE Proceedings Vol. 3480 (SPIE-International Society for Optical Engineering, Bellingham, Washington, 1998), p. 21.

[10] M. Mössle and R. Kleiner, Phys. Rev. B **59**, 4486 (1999).

[11] S. I. Woods *et al.,* IEEE Trans. Appl. Supercond. **9**, 3917 (1999).

[12] Z.-X. Shen *et al.,* Phys. Rev. Lett. **70**, 1553 (1993).

[13] T. Jacobs *et al.,* Phys. Rev. Lett. **75**, 4516 (1995).

[14] A. Yurgens *et al.,* Phys. Rev. Lett. **79**, 5122 (1997).

[15] R. Kleiner and P. Müller, Phys. Rev. B **49**, 1327 (1994).

[16] V. Ambegaokar and A. Baratoff, Phys. Rev. Lett. **10**, 486 (1963); **11**, 104 (1963).

[17] S. Massida, J. Yu, and A. J. Freeman, Physica (Amsterdam) **152C**, 251 (1988).

[18] J. Halbritter, J. Supercond. **11**, 231 (1998).